

Distribution Agreement

In presenting this thesis as a partial fulfillment of the requirements for an advanced degree from Emory University, I hereby grant to Emory University and its agents the non-exclusive license to archive, make accessible, and display my thesis or dissertation in whole or in part in all forms of media, now or hereafter known, including display on the world wide web. I understand that I may select some access restrictions as part of the online submission of this thesis or dissertation. I retain all ownership rights to the copyright of the thesis or dissertation. I also retain the right to use in future works (such as articles or books) all or part of this thesis.

Signature:

Jordan M. Sumliner

Date

Immobilization of Polyoxometalates for Electrochemical Water Oxidation

By

Jordan M. Sumliner

Master of Science

Chemistry

Craig L. Hill, Ph.D

Advisor

Cora E. MacBeth, Ph.D

Committee Member

R. Brian Dyer, Ph.D

Committee Member

Accepted:

Lisa A. Tedesco, Ph.D

Dean of the James T. Laney School of Graduate Studies

Date

Immobilization of Polyoxometalates for Electrochemical Water Oxidation

By

Jordan M. Sumliner

B.S., State University of New York at New Paltz, 2010

Advisor: Craig L. Hill, Ph.D

An abstract of a thesis submitted to the Faculty of the James T. Laney Graduate School
Studies of Emory University in partial fulfillment of the requirements for the degree of
Master of Science in Chemistry

2014

Abstract

Immobilization of Polyoxometalates for Electrochemical Water Oxidation

By Jordan M. Sumliner

Electrochemical cells capable of efficiently splitting water into its elemental constituents, H₂ and O₂, the former being a potent green fuel, are a significant area of scientific focus today. One important component of such a cell is the anode, which should be stable toward the harsh conditions needed for water oxidation. In addition, to overcome the exceedingly large overpotential required to oxidize water, a suitable catalyst, which is immobilized on the anode, is needed. In pursuit of these aims, the polyoxometalate water oxidation catalysts [Co₄(H₂O)₂(XW₉O₃₄)₂]¹⁰⁻, where X = V(V) and P(V) have been immobilized and characterized on various anode materials. In two different systems, the solubility of the immobilized catalyst was found to greatly influence its activity and stability. When the water soluble salt of [Co₄(H₂O)₂(PW₉O₃₄)₂]¹⁰⁻ is immobilized on cationic TiO₂ film anodes, and is used to oxidize water, the catalyst decomposes to an unknown cobalt oxide species. In another system, when water-insoluble [Co₄(H₂O)₂(VW₉O₃₄)₂]¹⁰⁻ is immobilized in a carbon paste anode, under turnover conditions, no catalyst decomposition is observed under turnover conditions, whereas a water-soluble salt of the same catalyst will decompose under these conditions.

Immobilization of Polyoxometalates for Electrochemical Water Oxidation

By

Jordan M. Sumliner

B.S., State University of New York at New Paltz, 2010

Advisor: Craig L. Hill, Ph.D

A thesis submitted to the Faculty of the James T. Laney Graduate School Studies of Emory University in partial fulfillment of the requirements for the degree of Master of Science in Chemistry

2014

Table of Contents

Abstract	iv
List of Abbreviations	vii
List of Figures	ix
List of Schemes	x
Chapter 1 General Introduction	1
Background.....	2
Polyoxometalates.....	5
POM WOCs.....	6
Chapter 2 Electrostatic Immobilization of $[\text{Co}_4(\text{H}_2\text{O})_2(\text{PW}_9\text{O}_{34})_2]^{10-}$ with the Viologen Bis(2-phosphonoethyl)-4,4'-bipyridinium	8
Introduction.....	9
Experimental	12
Results and Discussion.....	15
Conclusions	26
Chapter 3 Carbon Paste Electrodes for Water Oxidation: Immobilization of the WOC $[\text{Co}_4(\text{H}_2\text{O})_2(\text{VW}_9\text{O}_{34})_2]^{10-}$	27
Introduction.....	28
Experimental	30
Results and Discussion.....	32
Conclusions	40

References and Notes	41
----------------------------	----

List of Abbreviations

BE	Bulk electrolysis
bpy	2,2'-bipyridine
Co ₄ P ₂	[Co ₄ (H ₂ O) ₂ (PW ₉ O ₃₄) ₂] ¹⁰⁻
Co ₉ P ₅	[Co ₉ (H ₂ O) ₆ (OH) ₃ (HPO ₄) ₂ (PW ₉ O ₃₄) ₃] ¹⁶⁻
Co ₄ V ₂	[Co ₄ (H ₂ O) ₂ (VW ₉ O ₃₄) ₂] ¹⁰⁻
CPE	Carbon paste electrode
CV	Cyclic voltammetry
E	Potential
EVP ₂	Bis(2-phosphonoethyl)-4,4'-bipyridinium
EVP ₂ Cl ₂	Bis(2-phosphonoethyl)-4,4'-bipyridinium dichloride
FT-IR	Fourier transform infrared
FTO	Fluorine-doped tin oxide coated glass
GC	Gas chromatography
I	Current
MWCNTs	Multi-walled carbon nanotubes
PAMAM	Polyamidoamine ammonium
POM	Polyoxometalate

PV	Photovoltaic
RRDE	Rotating ring disk electrode
Ru_4Si_2	$[\{\text{Ru}_4\text{O}_4(\text{OH})_2(\text{H}_2\text{O})_4\}(\gamma\text{-SiW}_{10}\text{O}_{36})_2]^{10-}$
TBA	Tetrabutylammonium
UV-Vis	Ultraviolet-visible
WOC	Water oxidation catalyst
XPS	X-ray photoelectron spectroscopy
Zn_4P_2	$[\text{Zn}_4(\text{H}_2\text{O})_2(\text{PW}_9\text{O}_{34})_2]^{10-}$

List of Figures

Figure 2.1. Photograph of the one-compartment cell for bulk electrolysis. Co_4P_2 modified working electrode (left), Ag/AgCl (3 M NaCl) reference electrode (center) and Pt foil auxiliary electrode (right).....	14
Figure 2.2. CV trace of TiO_2 @FTO. Scan rate: 100 mV/s.....	17
Figure 2.3. CV trace of electrode 1 . Conditions: 0.1 M pH 8 sodium borate buffer, 0.2 M KCl, scan rate = 50 mV/s	18
Figure 2.4. CV traces of Co_4P_2 modified electrode 1 (red), Zn_4P_2 modified electrode 1 (orange), and unmodified electrode 1 (dashed black). Conditions: 0.1 M pH 8 sodium borate buffer, 0.5 M KNO_3 . Scan rate: 100 mV/s.....	21
Figure 2.5. XPS spectra series for Co_4P_2 modified electrode 1 before (top panels) and after (lower panels) one-hour BE at 1150 mV. The left panels are W 4f and the right panels are Co 2p.....	24
Figure 2.6. Electrochemical data series for Co_4P_2 modified electrode 1 . Panel A : one-hour bulk electrolyses at 1150 mV in the absence of 0.03 mM bpy. Panel B: one-hour bulk electrolysis at 1150 mV in the presence of bpy. Panel C: CV traces for electrode from Panel A, before (red) and after (blue) one-hour bulk electrolysis at 1150 mV. Panel (D): CV traces for electrode from Panel B, before (red) and after (blue) one-hour bulk electrolysis at 1150 mV. Note: The anodic limit was 1150 mV in the CV traces in Panel D. Scan rate: 50 mV/s for CV traces.....	25
Figure 3.1. CV traces for unmodified CPE (blue) and both Cs & TBA Co_4V_2 modified CPEs (red). Scan rate: 100 mV/s.....	34

Figure 3.2. Bulk electrolyses of TBA Co_4V_2 modified CPE first run (blue), second run (red) and of an unmodified CPE (green). The large spikes in the current are due to inefficient removal of $\text{O}_{2(g)}$ bubbles during the experiment.....35

Figure 3.3. FT-IR spectra of the TBA salt of Co_4V_2 pre-BE (black) and post-BE (red), extracted from the CPE.36

Figure 3.4. RDE CV traces of BASi CPE (blue) and ceresin wax modified CPE (red). Scan rate: 100 mV/s39

List of Schemes

Scheme 1.1. General scheme for a PV driven electrochemical water splitting cell. 4

Scheme 2.1. Immobilization of Co_4P_2 for electrochemical water oxidation. The positively charged viologen is covalently attached to TiO_2 and will attract the negatively charged POM molecules (not drawn to scale). 11

Chapter 1 General Introduction

Background

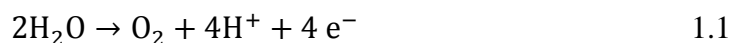
Current estimates suggest that that without direct intervention, our planet will succumb to two seemingly interlinked energy and climate change crises in the near future¹. One sought-after intervention is to use carbon-neutral energy sources, which are advantageous in both reducing our dependency on non-renewable energy sources, and limiting the overall amount of CO₂(g) emitted to the atmosphere. The consequences of the anthropogenic rise of CO₂(g) in the atmosphere could be linked to climate change, as past events have shown; despite some remaining uncertainty, action must be taken soon (within the next 10 years).¹

An obvious choice for a renewable energy source is sunlight, which has the ability to supply the world's current and future energy needs.² However, its capture and storage remain the two challenges imposed on wide-spread utilization³. Since sunlight is variable, diffuse and partially blocked by Earth's weather, the window of available solar energy is restricted. Once solar energy is captured, e.g. in a photovoltaic (PV) cell, where solar is converted to electricity via the photovoltaic effect, it must either be used immediately or stored for later use. In many circumstances, this is not ideal or possible.

One alternate utilization of solar energy with PV devices is through "solar fuel" generation, in a manner analogous to photosynthesis.⁴ Solar fuel utilizes renewable solar energy, in contrast to the majority of fuel in use today, which is generated from non-renewable energy sources. In general, fuel is a more energy dense storage medium for solar energy than batteries and a global infrastructure is currently in place to transport, handle and deliver various fuels. While plants photosynthesize simple sugars, a solar fuel for growth and maintenance, the potential target solar fuels for human use are H₂(g), CH₄(g)

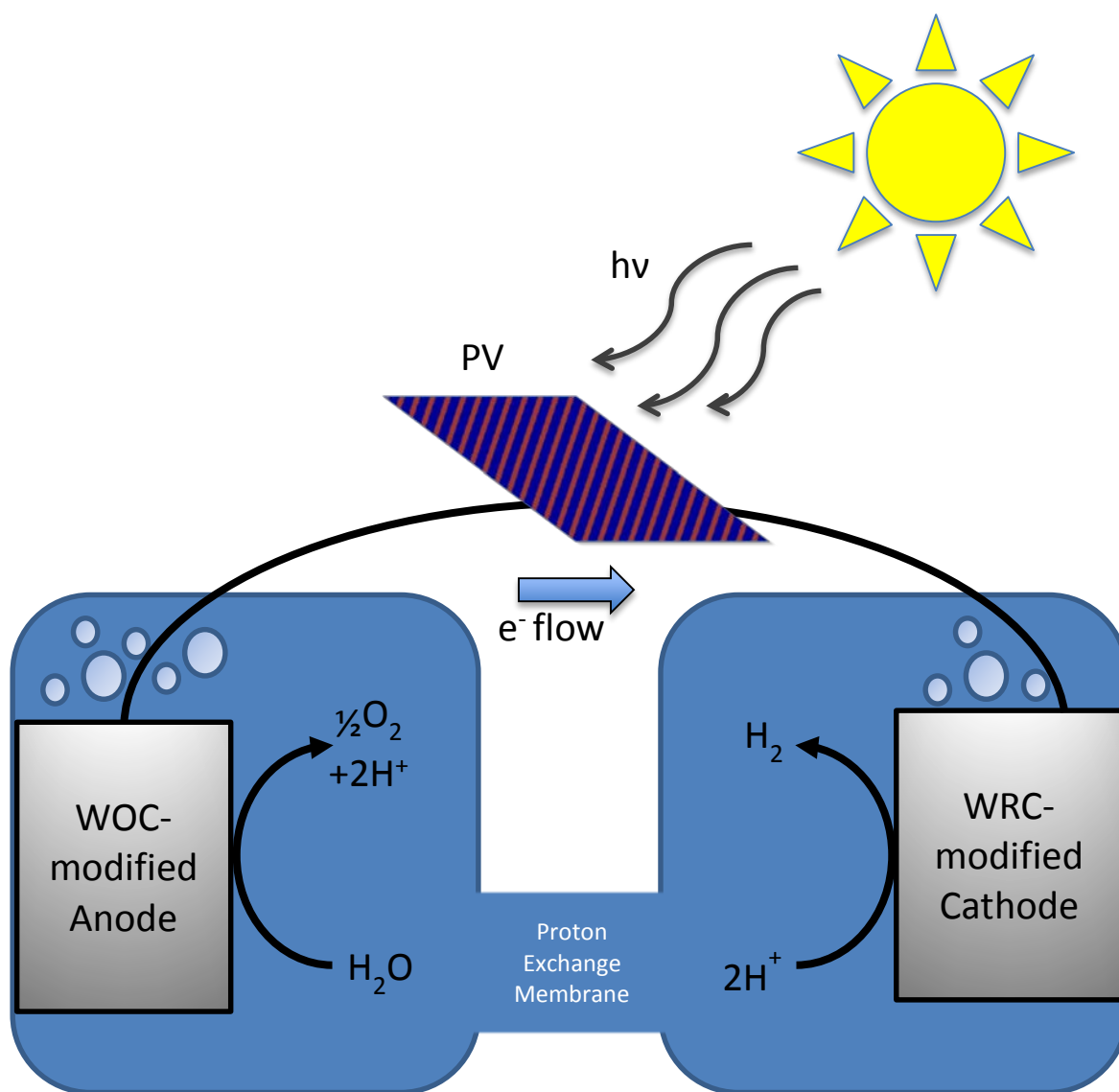
and CH_3OH .⁵ A monumental challenge to the scientific community then, is to design and build a device that is capable of solar fuel synthesis⁶. However, an alternate to a fully integrated device that can capture solar energy and convert it to fuel directly, would be to simply couple a traditional PV to an electrochemical cell, where fuel synthesis can take place.⁷

Toward development of an electrochemical cell capable of synthesizing solar fuel, catalysts are needed to decrease the high activation energies, or overpotentials, needed to drive fuel production. In the case of $\text{H}_2(\text{g})$ production, water splitting is represented by these two equations:



where Equation 1.1 takes place at the anode and Equation 1.2 takes place at the cathode of an electrochemical cell. At pH 0, the standard potential for Equation 1.1 is 1.23 V vs. NHE and 0.00 V vs. NHE for Equation 1.2; both reactions are pH dependent, as dictated by the Nernst equation. The standard potentials therefore change by -0.06 V per pH unit.

Such a cell is shown schematically in Scheme 1.1 and further clarity to the “modified electrodes” will be given in subsequent chapters. In general, such electrodes are ones to which a catalyst has been immobilized through either physical or chemical means. Specifically for water splitting, a WOC would be affixed to the anode and a WRC to the cathode. Significant effort has been made toward the development of WOCs and WRCs^{8,9}; the Hill group, alongside numerous other researchers, have investigated the use of polyoxometalates in this pursuit.¹⁰⁻¹⁵ Interest in POMs as WOCs and WRCs is better understood by briefly explaining some of their basic properties.



Scheme 1.1. General scheme for a PV driven electrochemical water splitting cell.

Polyoxometalates

POMs are discrete, soluble d-metal oxide clusters primarily composed of addenda metals M (e.g. W(VI), Mo(VI) and V(V) and seldom Nb(V) and Ta(V)).¹⁶ They are formed through acid condensation reactions and are readily tunable through incorporation of a heteroatom X (e.g. P(V), Si(IV), Al(III)), substitution of the addenda M with other transition metals (e.g. Co(II), V(V), Fe(III)) and by salt metathesis of their counterions. Through these modifications, an extensive family of POMs have been produced, carefully characterized with a variety of spectroscopic techniques (e.g. X-ray crystallography, FT-IR, UV-vis, NMR) and have frequently been employed in catalytic applications.^{17,18}

In addition to these studies, the electrochemical properties of POMs have made them targets of extensive voltammetric studies and electrocatalytic oxidations and reductions.¹⁹ Early work (late 1960s through mid-1970s) by Pope and co-workers²⁰⁻²⁵ found that multiple reducing equivalents (electrons) could be stored in Keggin and Dawson POMs and these “heteropoly blues” could be characterized by UV-vis due to inter-valence charge transfer bands between the addenda metals. These reduction processes are usually accompanied by protonation of the more basic oxygen centers as the POM overall becomes more basic upon reduction, but reduction is strongly dependent on the conditions (pH, electrolyte & solvent)²⁶ as well as the POM and its counterions.²⁷

Later electrochemical studies with POMs (1980s and 1990s) examined on their use as electrocatalysts for H^+ , NO_3^- , ClO_3^- and O_2 reduction, where the POM acts as a mediator for the reduction reaction.¹⁹ This type of reactivity was exploited for sensitive,

amperometric sensors.²⁸ For oxidation reactions, substituted transition metal(s) (Co(II), Ru(IV), etc) are considered to be the active site(s) and the reaction proceeds through oxidation of the metal site, followed by oxidation of the substrate by the POM.

Often, these studies have noted that POMs spontaneously adsorb to the electrode, modifying it strongly enough that simple rinsing with solvent would not dislodge the POM.²⁹ The cause of this adsorption phenomenon was not clear and continues to be poorly understood, as it is dependent on the electrode material, the solution conditions, and the POM as well.¹⁹ However, this phenomenon has been exploited for electrochemical catalytic reactions over the past 30 years. A detailed review of the field up to 1998 can be found in reference 19.

POM WOCs

In 2008, the POM $[\{\text{Ru}_4\text{O}_4(\text{OH})_2(\text{H}_2\text{O})_4\}(\gamma\text{-SiW}_{10}\text{O}_{36})_2]^{10-}$, simultaneously discovered by the Hill group and the Bonchio group, was shown to be a WOC in electrochemical, chemical and photochemical schemes¹⁵. Bonchio's group, along with the Bond group have exploited the rich electrochemistry of the POM and immobilized it on various electrode materials.³⁰⁻³² This POM sparked thorough studies into the POMs as WOCs^{9,14} and brought forth much needed scrutiny to the field of WOCs in general.^{33,34}

In general, the specific reaction conditions used in a WOC study are key toward supporting the authors claim of catalyst stability, and POM WOCs are no exception.³⁵⁻⁴⁵ Perhaps the most fitting phrase that can succinctly sum up these studies is "conditions matter", the primary example in the field of POM WOCs being $[\text{Co}_4(\text{H}_2\text{O})_2(\text{PW}_9\text{O}_{34})_2]^{10-}$.

In multiple, unique investigations^{11,36-39,43,45-48}, this POM was found to be either be stable, unstable, and/or the observed catalytic activity could be accounted for by decomposition products of the parent POM. These studies made it imperative that the question “Is Co_4P_2 an authentic, molecular WOC?” be addressed head-on, the ultimate result being that “conditions matter” when it comes to POM WOCs and WOCs in general.³⁷ Most relevant to the work described here, is that found Co_4P_2 *is not* an authentic, molecular WOC when employed as an electrochemical WOC.^{36,38} The efforts described in Chapter 2, to immobilize Co_4P_2 on an electrode for electrochemical water oxidation, confirm this conclusion, and highlight the difficulty in studying electrochemical WOCs that are immobilized on an electrode surface. In Chapter 3, another approach toward WOC immobilization is discussed, with the POM $[\text{Co}_4(\text{H}_2\text{O})_2(\text{VW}_9\text{O}_{34})_2]^{10-}$.

**Chapter 2 Electrostatic Immobilization of
[Co₄(H₂O)₂(PW₉O₃₄)₂]¹⁰⁻ with the Viologen Bis(2-
phosphonoethyl)-4,4'-bipyridinium**

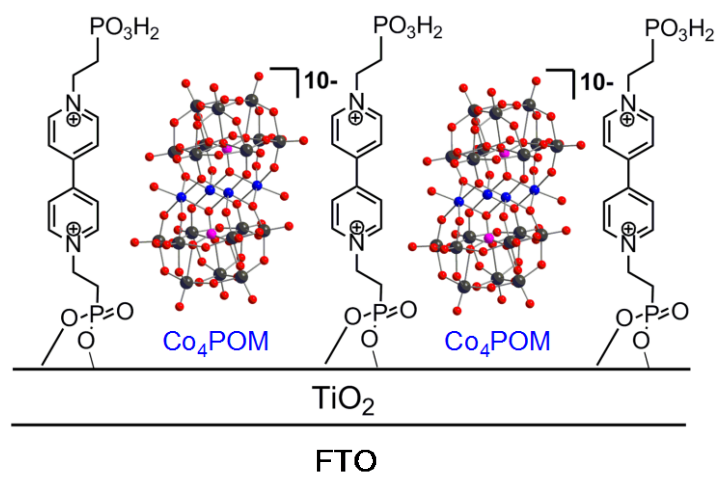
Introduction

Immobilization of POMs on electrode surfaces for electro- and photo-catalytic applications has been explored over the past 30 years. A variety of approaches have been developed, including electrostatic modification. Here, a surface is modified with a cation, which strongly attracts the anionic POM. A semiconductor metal oxide film provides a stable and cation-modifiable surface to support molecular catalysts. TiO_2 , one of the most studied semiconductor metal oxides, has been used in various electro- and photo-catalytic applications, dye sensitized solar cells, and in electrochromic devices.⁴⁹ In these systems, molecules are immobilized to the surface of the oxide through strong covalent bonds. One class of compounds that has been used in such a way is the viologens, which have appeared in commercial EC devices.^{50,51} Viologens are readily modifiable through simple $\text{S}_{\text{N}}2$ type chemistry, where a strong nucleophile attacks the 4,4'-bipyridine precursor.⁵² A range of available nucleophiles has yielded a rich family of viologens to investigate, and in particular their electrochemistry.⁵¹ When functionalized with acid linker groups, such as phosphonate or carboxylate, TiO_2 can be modified with a viologen, and due to the positive charge on the viologen, negatively charged POMs can be immobilized on the resulting surface. TiO_2 can be deposited on FTO, to generate TiO_2 film electrodes, which, upon modification with a viologen, immobilize POMs.

This approach toward POM immobilization, involving an oppositely charged surface, has been employed in the past under various reaction conditions with varying degrees of success, usually governed by the stability of the POM itself.⁵³ One noteworthy and inspiring example was published by Bonchio group in 2010.³¹ In this case, the Ru_4Si_2 POM was immobilized on PAMAM modified MWCNTs, which, due to their positive

charge, were able to support the negatively charged POM. This material was then dropcast (a small amount of material dispersed in a solvent is pipetted) on an FTO electrode, and found to oxidize water efficiently under electrochemical bias. Spectroscopic evidence confirmed that the POM was intact upon immobilization, and current versus time measurements lent support to the conclusion that the POM was stable following water oxidation electrolysis.

The work herein to be described builds upon this approach, but with viologen modified TiO₂-film electrodes in place of the modified MWCNTs, as shown in Scheme 2.1, incorporating the Co₄P₂ WOC. Co₄P₂ was chosen for this study because it was at the time the fastest molecular WOC reported and a purported electrochemical WOC. However, this POM was shown to be unstable under electrochemical bias, and would go on to form another WOC, CoO_x, thus complicating its study on an electrode surface. This finding is supported by another report on the electrochemical behavior of this WOC.³⁶



Scheme 2.1. Immobilization of Co₄P₂ for electrochemical water oxidation. The positively charged viologen is covalently attached to TiO₂ and will attract the negatively charged POM molecules (not drawn to scale).

Experimental

Bis(2-phosphonoethyl)-4,4'-bipyridinium dichloride (EVP_2Cl_2) was prepared following the literature method and its identity and purity were confirmed by $^1\text{H-NMR}$ spectroscopy.⁵⁰ The POMs, $\text{Na}_{10}[\text{Co}_4(\text{H}_2\text{O})_2(\text{PW}_9\text{O}_{34})_2]$ (Co_4P_2) and $\text{Na}_{10}[\text{Zn}_4(\text{H}_2\text{O})_2(\text{PW}_9\text{O}_{34})_2]$ (Zn_4P_2), were provided by the Hill group and their purities and identities were confirmed by FT-IR spectroscopy.

TiO_2 film electrodes were prepared following a literature method.⁵⁴ Briefly, FTO glass (Hartford Glass Co.) was cleaned by sonication in both acetone and ethanol, allowed to dry, then masked with Scotch® tape, which also controlled the film thickness. Colloidal TiO_2 was spread on cleaned FTO glass, allowed to air dry, then calcined in a furnace at 400°C for 2 h (heating rate $2^\circ\text{C}/\text{min}$).

XPS measurements were conducted by Walter Henderson at Georgia Tech, with a Thermo Scientific K-Alpha XPS system equipped with an Al anode. The typical spot diameter for the measurement was $400\ \mu\text{m}$. For quantification of the POM, the areas under the W(VI) 4f peaks and Co(II) 2p peaks were integrated and corrected based on the sensitivity factor provided from the instrument.

Modification of TiO_2 film electrodes was accomplished via the alternate dip method.⁵³ Briefly, films were dipped into an aqueous solution of 0.02 M EVP_2Cl_2 for 24 h, then rinsed with DI water and allowed to air dry for at least 12 h. POMs were immobilized on the EVP_2 modified TiO_2 film electrodes in the same manner.

Electrochemical measurements were conducted with a BASi CV-50W potentiostat, Ag/AgCl (3 M NaCl) reference electrode and either a Pt wire or foil auxiliary electrode. Electrochemical data has been plotted in the “European” convention, where anodic current

is “positive” and cathodic current is “negative”. Cyclic voltammetry was conducted in a one-compartment cell. Typically, the solution was purged with Ar(g) for at least 10 minutes, then kept under a positive pressure of Ar(g) during the experiment. If not otherwise specified, pH 8 sodium borate buffer (100 mM) + 200 mM NaClO₄ was used as the electrolyte.

Spectroelectrochemical measurements were performed with an Agilent 8453 UV-vis spectrophotometer in a 1 cm pathlength polystyrene cuvette. The solution was purged in a similar manner as in CV experiments, then kept under a positive pressure of Ar(g).

Bulk electrolyses were conducted in an air-tight one-compartment cell. The working electrode was attached to a copper wire lead via conductive-epoxy; the exposed conductive epoxy was coated with a non-conductive epoxy to prevent an undesired reaction. The electrode leads for the working and auxiliary electrodes were feed through rubber septa fitted in the cell top. Typically, 25 mL of solution was added to the cell, then the whole cell was purged with Ar(g) for at least 30 min to remove dissolved O₂(g). Oxygen measurements were made by GC headspace analysis, as previously described.⁴⁸ The one-compartment cell was calibrated for both H₂(g) and O₂(g) with a method previously described.¹¹



Figure 2.1. Photograph of the one-compartment cell for bulk electrolysis. Co_4P_2 modified working electrode (left), Ag/AgCl (3 M NaCl) reference electrode (center) and Pt foil auxiliary electrode (right).

Results and Discussion

Bare, unmodified TiO₂ film electrodes give a featureless CV within the potential range shown in Figure 2.2, in buffered and buffer-free electrolyte. Upon modification of TiO₂ with EVP₂ (electrode **1**), a noticeable reduction process is observed, which is assigned to a 1 e⁻ reduction to the radical EVP₂^{•+} species, along with the appearance of a dark violet color on the film⁵¹. When the potential is cycled back, the violet color fades, which suggests a reversible reduction. However, the reversible wave is partly obscured by an independent TiO₂ capacitance current⁵⁵ (not shown).

The reduction process for EVP₂ shown in Figure 2.3 as a reversible, surface bound species⁵⁶, is pH dependent, and the stability of the linkage is buffer dependent (see Table 2.1), indicating that the phosphonate groups are at least partially bound to TiO₂. The buffer-dependent stability bears a striking similarity to the stability woes of [Ru(bpy)₂(X₂-bpy)]²⁺, where X = COOH, PO₃H₂, complexes^{54,57,58} bound on TiO₂ films, in that phosphate anions competitively bind against the dye molecules, thereby slowly displacing them. UV-Vis spectroelectrochemical experiments where electrode **1** was held at -700 mV, sufficient for reduction, gave a UV-vis spectrum that matched the literature⁵⁰, which confirmed that the electrode was modified with EVP₂.

POM modified electrodes were prepared using electrode **1** by an extended dip coating method. Dip coating is widely used to modify electrodes with POMs and other charged species.²⁸ It is important to thoroughly rinse the dipped electrodes with water to ensure that only strongly bound species are left on the electrode surface.

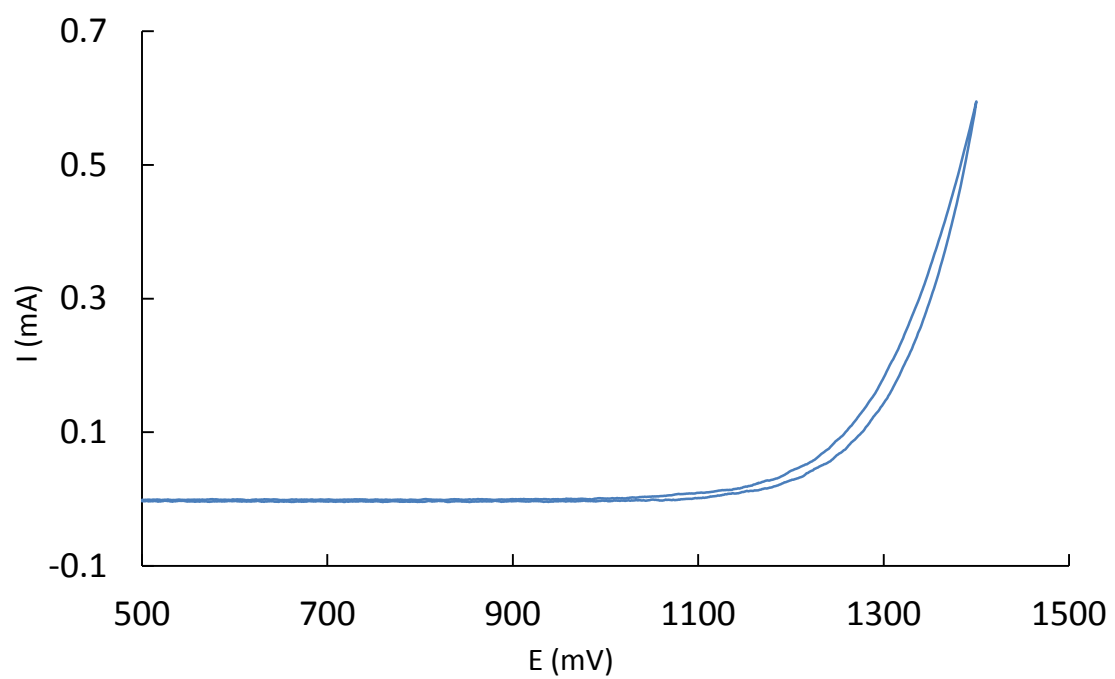


Figure 2.2. CV trace of TiO₂@FTO. Scan rate: 100 mV/s

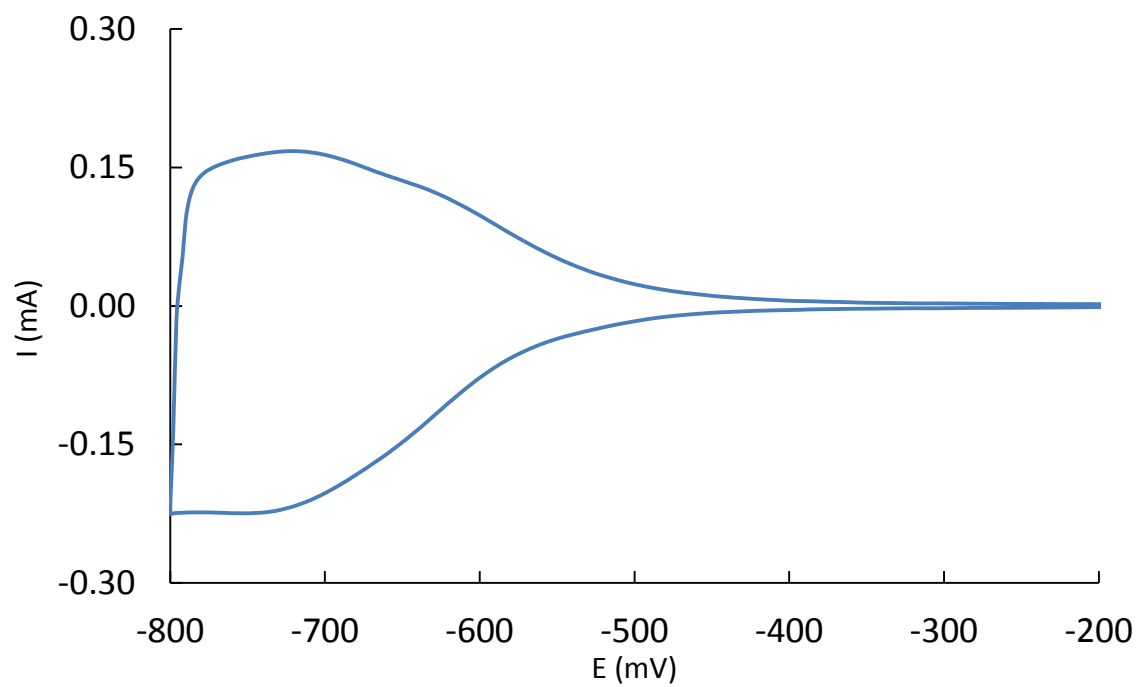


Figure 2.3. CV trace of electrode **1**. Conditions: 0.1 M pH 8 sodium borate buffer, 0.2 M KCl, scan rate = 50 mV/s

Entry	Conditions	E_{red} (mV)	Stable	Note
1	0.1 M pH 8 borate buffer	-700	Yes	~5% decrease in current after 12 h soak.
2	0.1 M pH 8 phosphate buffer	-720	No	Complete desorption of EVP ₂ after 12 h
3	0.1 M pH 7 phosphate buffer	-620	No	Complete desorption of EVP ₂ after 12 h
4	0.1 M pH 5 acetate buffer	-450	Yes	No change in current after 12 h soak.

Table 2.1. Effect of buffer conditions on hydrolytic stability of electrode **1** and reduction potential of EVP₂.

While the formation of highly reduced POM species, or “heteropoly blues” is well documented, it is generally limited to acidic pH (<5), where the POM is partially protonated.¹⁶

Under the conditions used in this study (pH 7-8), these reduction processes were not observed for Co_4P_2 , or for Zn_4P_2 and were also possibly obscured by the reduction of EVP_2 and the capacitive, charging process for TiO_2 . Another, perhaps expected, consequence of POM immobilization is a shift in the reduction potential of EVP_2 by approximately 60 mV; an effect due to the ability of the POM to act as a base under these conditions.⁵⁹ Upon immobilization of Co_4P_2 via the dip coating method, its CV was obtained under standard conditions and found to give a catalytic wave for water oxidation, well below that of the unmodified electrode **1** as shown in Figure 2.4. When the structurally analogous, but redox inactive Zn_4P_2 was immobilized on electrode **1**, no such wave was observed.

Now, a brief interlude will be given on M_4P_2 ($\text{M} = \text{Co}, \text{Zn}$) electrochemistry and stability, which will hopefully better prepare the reader for the following section. The electrochemical properties of the “sandwich-type” POMs are poorly understood, especially when compared to their Keggin parents.¹⁹ Of the few reports that have investigated the electrochemistry of these sandwich-type POMs, no satisfactory explanation has been given as to why, under aqueous conditions but not non-aqueous conditions, Co(II)/(III) is voltammetrically silent.^{60,61} Thus, CV and related experiments *alone can provide only limited insight* into the electrochemical behavior of these POMs.

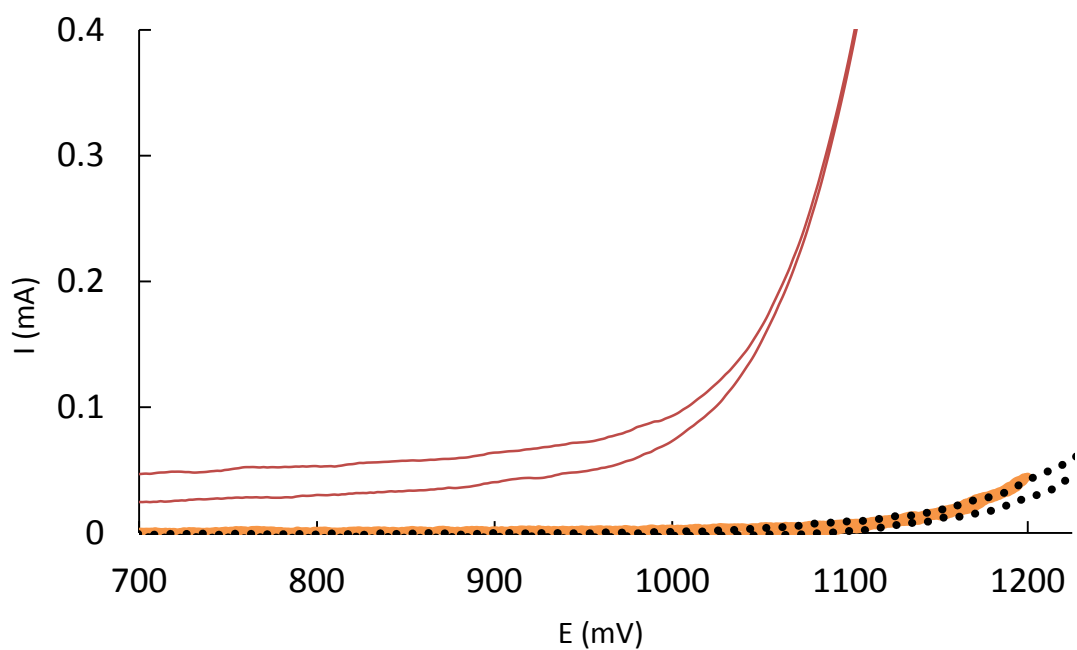


Figure 2.4. CV traces of Co₄P₂ modified electrode **1** (red), Zn₄P₂ modified electrode **1** (orange), and unmodified electrode **1** (dashed black). Conditions: 0.1 M pH 8 sodium borate buffer, 0.5 M KNO₃. Scan rate: 100 mV/s

When Co_4P_2 was reported to be a homogeneous WOC *with the chemical oxidant* $\text{Ru}(\text{bpy})_3^{3+}$, a thorough electrochemical investigation of its electrochemical WOC properties had not yet been reported. Contemporaneous work by Stracke and Finke found that when Co_4P_2 was used in pH 8 phosphate buffer as an electrochemical WOC, it would either: a) decompose to form electrodeposited cobalt oxide³⁶, or b) give indistinguishable catalytic activity from partially hydrolyzed $\text{Co}^{2+}(\text{aq})$ ³⁸. Their findings set off an intensive study³⁷ of the stability of Co_4P_2 under two separate sets of conditions reported by the Hill group^{11,48}, and changed the focus of this work toward understanding the stability of Co_4P_2 when immobilized on electrode **1**.

Several attempts to use FT-IR and UV-Vis to spectroscopically detect Co_4P_2 failed and only X-ray photoelectron spectroscopy could detect and quantify Co_4P_2 on EVP_2 TiO_2 film electrodes. XPS analysis shown in Figure 2.5, top panels, on a freshly prepared Co_4P_2 modified electrode gave a Co:W ratio of 2:9, which matches the expected elemental composition of the POM and confirmed that the POM was immobilized on the surface. The binding energies for the Co 2p, P 2p and W 4f were within the range of known binding energies for Co(II), P(V) and W(VI), respectively, in similar POMs.^{62,63}

Bulk electrolysis (BE) for water oxidation with Co_4P_2 modified electrodes gave two results: $\text{O}_2(\text{g})$ and $\text{H}_2(\text{g})$ are generated with a Faradaic efficiency ~60% but, perhaps more importantly, the catalytic current *increased* during the experiment (Figure 2.6, Panel A).⁶⁴ The former result confirmed that water oxidation does occur at Co_4P_2 modified electrode **1**. The latter result was further investigated with CV and XPS, since an increase in current alone does not signal catalyst instability. The CV trace for the Co_4P_2 modified electrodes, post BE, gave a higher current response for potentials >900 mV, which did support the

formation of a more active catalytic species for water oxidation (Figure 2.6, Panel C). In addition, the XPS analysis of a post-BE electrode revealed that the Co:W ratio decreased to 0.5:9, which suggested that 2 Co^{2+} per POM were absent from the electrode surface, and confirmed instability of the POM during water oxidation (Figure 2.5, lower panels). These results indicate that Co_4P_2 decomposes during BE, to form a more active catalytic species. Due to the observed decomposition process, no derived catalytic values such as the TON or TOF could be effectively calculated.

To probe how Co_4P_2 modified electrode **1** decomposed to form such a species, a chemical chelator, 2,2'-bipyridine (bpy), was used, which effectively scavenges $\text{Co}^{2+}(\text{aq})$ under the experimental conditions.^{11,45} Whereas Stracke and Finke found that aging 0.5 mM Co_4P_2 in 100 mM pH 8 sodium phosphate buffer allowed released $\text{Co}^{2+}(\text{aq})$ from the POM to form catalytically active electrode films³⁶, a series of electrochemical experiments presented here found that bpy prevents the formation of free $\text{Co}^{2+}(\text{aq})$ and film formation. CV revealed that Co_4P_2 aged under the same set of conditions, but in the presence of 0.3 mM bpy, does not give catalytically active electrode films. Instead, a precipitate forms, which was identified as $[\text{Co}(\text{bpy})_3]^{2+}$ by FT-IR analysis (not shown). When BE at 1150 mV was performed in the presence of bpy, the catalytic current for water oxidation will reach a steady state in its presence. The overall catalytic current is smaller in the presence of bpy as well, and this current likely represents the actual activity of the POM. A similar series of experiments performed with the related Co_9P_5 POM WOC, which behaves analogously to Co_4P_2 , gave similar results.⁴⁵

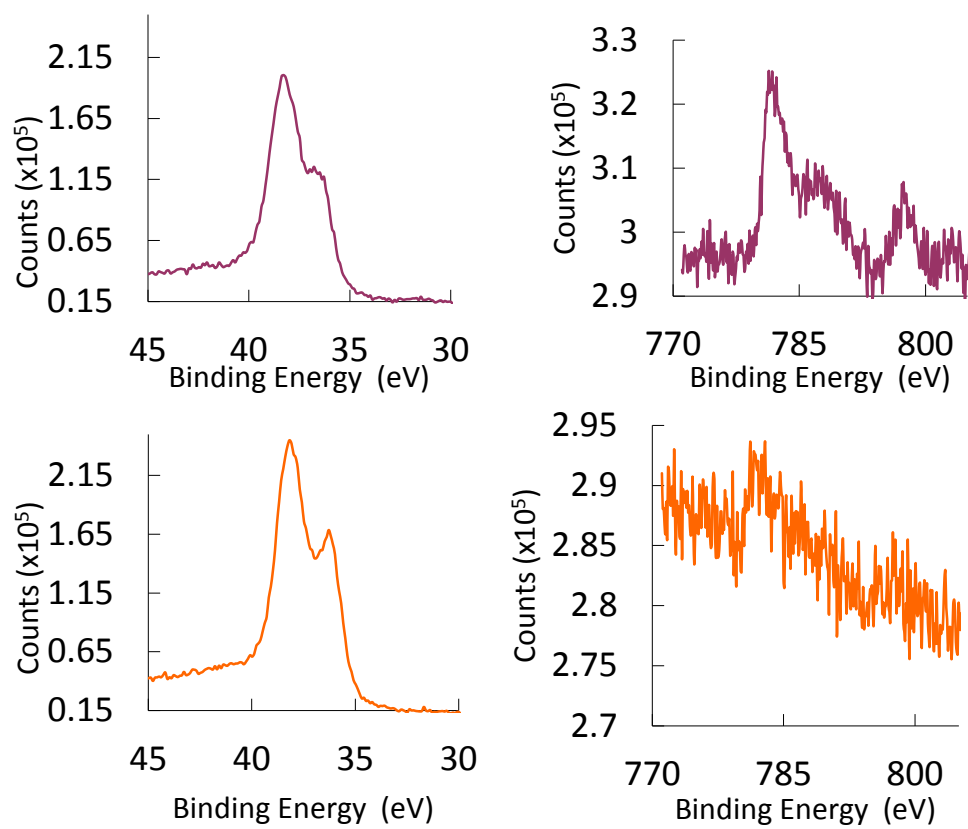


Figure 2.5. XPS spectra series for Co_4P_2 modified electrode **1** before (top panels) and after (lower panels) one-hour BE at 1150 mV. The left panels are W 4f and the right panels are Co 2p.

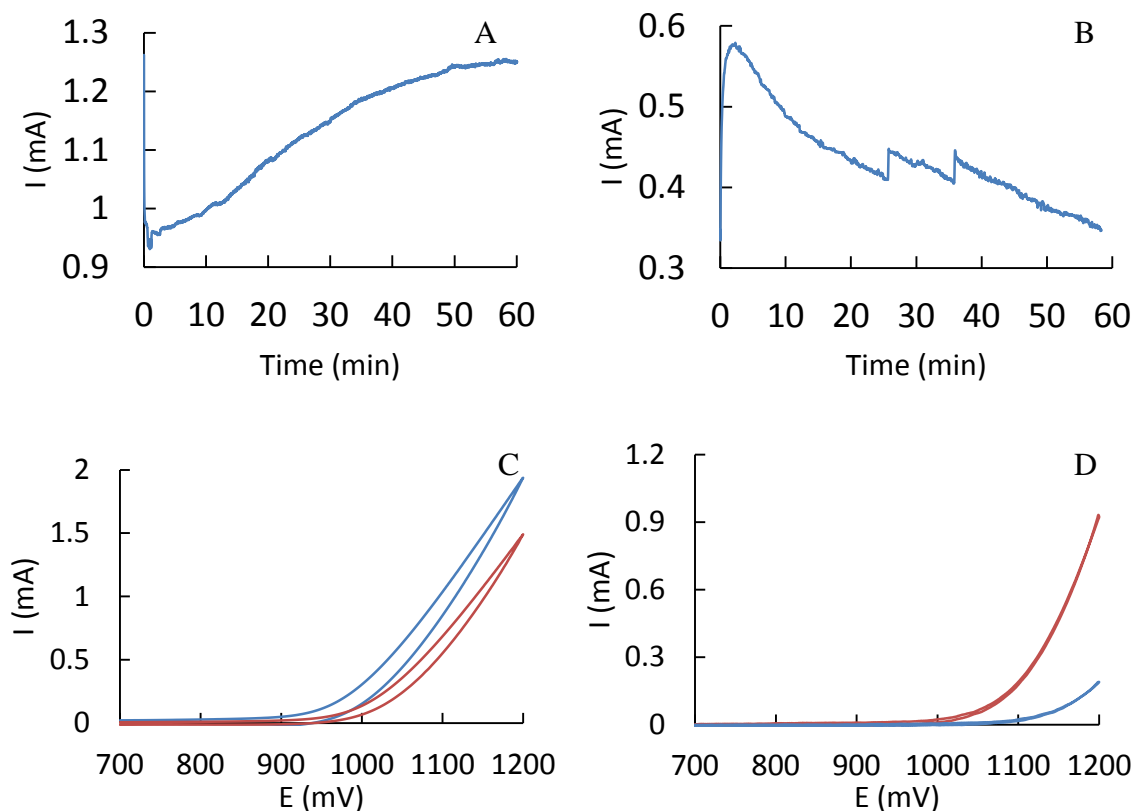


Figure 2.6. Electrochemical data series for Co_4P_2 modified electrode **1**. Panel A : one-hour bulk electrolyses at 1150 mV in the absence of 0.03 mM bpy. Panel B: one-hour bulk electrolysis at 1150 mV in the presence of bpy. Panel C: CV traces for electrode from Panel A, before (red) and after (blue) one-hour bulk electrolysis at 1150 mV. Panel (D): CV traces for electrode from Panel B, before (red) and after (blue) one-hour bulk electrolysis at 1150 mV. Note: The anodic limit was 1150 mV in the CV traces in Panel D. Scan rate: 50 mV/s for CV traces.

In the more complicated Co_4P_2 modified electrode **1** case, CV and BE experiments again provide strong evidence to suggest that the electrodes decompose via a similar route. In Figure 2.6, Panels B & D, the influence of bpy on the behavior of the electrode is clearly observed. Whereas the catalytic current for the electrode was found to increase during the course of BE at 1150 mV, the opposite is true when the experiment was performed in the presence of 0.03 mM bpy (Figure 2.6, Panel B). The CV traces before and after the BE experiment also show this decrease in current (Figure 2.6, Panel D), in agreement with the behavior of Co_4P_2 in solution.

Conclusions

Electrostatic immobilization of POMs on cationic electrode surfaces can be a promising approach toward POM-modified surfaces, however the POM itself must be stable under the experimental conditions utilized. In the case of Co_4P_2 on EVP_2 modified TiO_2 electrodes, the hydrolytic instability of the POM allows for the formation of catalytically active CoO_x species, which overshadows the POM's electrochemical WOC performance. Until a more hydrolytically stable POM WOC is found, this electrostatic immobilization is a poor choice toward the development of a WOC anode.

**Chapter 3 Carbon Paste Electrodes for Water Oxidation:
Immobilization of the WOC $[\text{Co}_4(\text{H}_2\text{O})_2(\text{VW}_9\text{O}_{34})_2]^{10-}$**

Introduction

Carbon paste electrodes (CPEs) were first reported in the late 1950s from the Adams Laboratory⁶⁵, and since then, have developed into a popular electrode material.⁶⁶ Carbon pastes are constructed by mechanically mixing a micron-particle carbon powder, usually graphite, with a binder, usually paraffin oil, in a mortar and pestle. The paste is then loaded into an electrode body, which contains a cavity, in place of the solid electrode material (gold, glassy carbon, platinum etc.). The varieties of carbon paste formulations available and electrode body designs, the ability to modify the CPE, and its relatively low cost, have all contributed to their widespread use.

As alluded to in the previous chapter, modification of an electrode surface with a molecular catalyst or catalyst material (network solid, amorphous metal oxide etc.) has been and continues to be well studied.⁶⁷ CPEs are no exception to this and have been modified with various catalysts. In practice however, the intention of the catalyst was to enhance a detection limit with an electrochemical sensor⁶⁶ rather than in bulk (exhaustive) electrolyses.

Immobilization of POMs in CPEs was first reported in 2005⁶⁸ with $[\text{PMo}_{12}\text{O}_{40}]^{3-}$ and since then, several papers have followed.^{69,70} These electrodes were employed as sensors for nitrate and other reducible analytes, due to the POM's ability to catalyze this electroreduction process¹⁹. Keggin-type POMs remain the most commonly used members of the large POM family, and their use in CPEs is no exception. Due to their overall low negative charge density, they tend to be very water-soluble, which presents a challenge to immobilization. Recently, the cesium salt of the POM WOC $[\text{Co}_9(\text{H}_2\text{O})_6(\text{OH})_3(\text{HPO}_4)_2(\text{PW}_9\text{O}_{34})_3]^{16-}$ was immobilized in a CPE for water oxidation at

relatively high overpotentials.⁷⁰ A key benchmark of a WOC is the overpotential required for it to drive Equation 1.1 at the anode. The overpotential is the applied potential in addition to the thermodynamic potential for a reaction.⁵⁶ Jaramillo, Peters and McCrory et al. set an ambitious maximum overpotential range for heterogeneous WOCs between 0.35 and 0.43 V⁷¹, which Co₉P₅ far exceeds. The stability of Co₉P₅ under turnover conditions for electrochemical water oxidation was previously addressed during the initial investigation of the water-soluble salt⁴⁵ but it was shown that in the presence of bpy as a chelator, that POM was an authentic electrochemical WOC. In contrast, the immobilized, insoluble cesium salt of this POM could be used in the absence of any chelator, which implies that its stability as a WOC is attributed to its apparent insolubility.

An alternative approach to POM immobilization is through hydrophobic interactions between the POM salt and the electrode. Simple salt metathesis of the water-soluble POM salt, with a hydrophobic quaternary ammonium salt, such as TBA, yields a water-insoluble POM salt.⁷² This approach has yielded POM-functionalized nanomaterials that are capable of catalyzing chemical oxidation of C-H bonds, alcohols and sulfides.⁷³

Here, the TBA salt of Co₄V₂ has been immobilized in a CPE, yielding a functionalized anode for water oxidation. The CPE serves the role as a conductive support for the otherwise non-conductive POM salt. Electrochemical studies of the POM-CPE revealed that the POM does not decompose to form the catalytically active CoO_x species, and spectroscopic techniques confirm that no other POM species is formed after water oxidation catalysis. However, under the experimental conditions for water oxidation catalysis, the CPE alone was found to oxidize water as well, albeit with a lower current. To

explore this unexpected property of the CPE, a different CPE formulation was tested that gave lower activity for electrochemical water oxidation.

Experimental

Both $\text{Cs}_{10}[\text{Co}_4(\text{H}_2\text{O})_2(\text{VW}_9\text{O}_{34})_2]$ and $\text{TBA}_{10}[\text{Co}_4(\text{H}_2\text{O})_2(\text{VW}_9\text{O}_{34})_2]$ were prepared through salt metathesis from the parent $\text{Na}_{10}[\text{Co}_4(\text{H}_2\text{O})_2(\text{VW}_9\text{O}_{34})_2]$.¹² The purities of the prepared POMs were confirmed by either FT-IR & elemental analysis (cesium salt), or FT-IR & ^{51}V -NMR (TBA salt).

Carbon paste electrodes were prepared with either BASi carbon paste oil (CF-1010) or with the ceresin wax-impregnated carbon paste described below. For control experiments, the carbon paste was simply packed into a BASi carbon paste electrode body (MF-2010), and the surface smoothed on an index-sized paper card. To prepare POM modified carbon paste electrodes, the appropriate amount of POM (typically 10% w/w) was weighed along with the carbon paste, then transferred to an agate mortar and homogenized with an agate pestle. The agate was found to be superior to porcelain, as it did not adsorb the carbon paste and could be easily cleaned.

Electrochemical experiments were performed with a Pine WaveDriver 20 bipotentiostat, and unless otherwise specified, 80 mM pH 8 sodium borate buffer with 200 mM sodium perchlorate was used as the electrolyte. The reference electrode was Ag/AgCl (3 M NaCl) and the auxiliary electrode was either a short platinum wire (3 cm) or coil (10 cm). Cyclic voltammetry was performed in a one-compartment three-electrode cell. Rotating disk electrode CV experiments were conducted at 1000 RPM, in a Pine 150 mL cell for rotating electrodes, with a Pine E6 Series ChangeDisk RRDE tip equipped with a

custom made well for carbon paste as the working electrode. Controlled potential electrolysis was performed in a custom-built gas-tight-two-compartment cell (Tudor Scientific) with a Nafion® membrane separating the working and auxiliary compartments. The cell body was fitted to the cap with a ground glass joint and the cap contained two Ace®-threaded #7 joints and a 14/20 ground glass joint. The working and reference electrodes were fitted into the Ace®-threaded joints and a septum was placed into the ground glass joint.

Prior to the start of the experiments where $O_2(g)$ was quantified, the working compartment was purged with $Ar(g)$ for at least 30 minutes to remove dissolved $O_2(g)$. The working electrode was not placed into the electrolyte until after sealing the cell. Oxygen measurements were made by GC headspace analysis, as previously described⁴⁸. The working compartment in the cell was calibrated for $O_2(g)$.

Extraction of the TBA salt of Co_4V_2 from carbon paste, either pre- or post- bulk electrolysis was conducted as follows: the paste was removed from the electrode body via sonication in toluene. The POM was precipitated out by additional of 2,2-diethyl ether, while the paraffin binder oil was left in the toluene. The precipitate was dried under air and weighed to confirm no % change in mass before or after the bulk electrolysis. With a separate sample, a KBr pellet was prepared from the dried precipitate (3% w/w) to confirm the stability of the POM by FT-IR. Finally, another sample was used to prepare a ^{51}V -NMR sample, similar to the method described in Lv et al.¹²

Results and Discussion

Modification of the CPE with either the Cs or TBA salts of Co_4V_2 significantly enhances the catalytic current for water oxidation, as observed by CV. Like with Co_4P_2 , aside from a catalytic wave, no other observable voltammetric features for Co_4V_2 are present within this potential window (Figure 3.1). The observed shape of the catalytic wave for the Co_4V_2 modified CPE (10% w/w) reaches a plateau at around 1200 mV, upon which the water oxidation process becomes diffusion-controlled. The thermodynamic potential for water oxidation, Equation 1.1, at pH 8 is 0.55 V vs Ag/AgCl (3 M NaCl), however the overpotential required for Co_4V_2 is ~ 0.75 V.

Bulk electrolyses (BE) at 1300 mV, with 10% w/w Co_4V_2 modified CPE, confirmed that water oxidation is the dominant reaction in the system, with a Faradaic efficiency approaching 100% for $\text{O}_2(\text{g})$. A TON of 20, where TON is defined as final moles O_2 / total moles catalyst, was calculated for the Co_4V_2 modified CPE. The current vs. time profile for a first run CPE gave a noticeable rise in current during the first hour of electrolysis, followed by a steady state current (Figure 3.2). Subsequent BEs with the same CPE gave no noticeable increase in current during the same period of time, which suggested that the increase could be due to transformation of the catalyst to another species. Due to the propensity of Co_4P_2 to decompose to CoO_x species when used on or at an electrode surface, it was necessary to carefully determine whether Co_4V_2 decomposes in the CPE.

Three lines of evidence support the claim that Co_4V_2 is *stable and does not decompose to any CoO_x species or any other POM* under this set of experimental conditions. First, the POM salt can be quantitatively extracted out from the CPE before and

after use in a bulk electrolysis experiment, which implies no catalyst loss. This result was further corroborated by FT-IR and solution state ^{51}V -NMR analysis of the extracted salt, in which no changes in the POM framework were observed. The FT-IR spectra of the TBA salt of Co_4V_2 pre- and post- extraction are shown in Figure 3.3 and no significant differences could be discerned between these spectra in the main stretching and bending modes of the POM between the region of 650 and 1000 cm^{-1} , although a difference spectrum could be used to show 100% stability of the POM. The ^{51}V -NMR shift for Co_4V_2 is unaffected after BE experiments from the CPE, and no other V-containing species were observed by this method (not shown).

These results seem striking in light of the thorough work done on Co_4P_2 , so let it be further discussed here. A key difference here may be that the TBA counterions prevent the parent POM from decomposition. The exact reason for this is not entirely known, but could be attributed to the complete insolubility of the TBA Co_4V_2 salt in water. Along this line of reasoning, one preliminary step in the decomposition of the Co_4X_2 POMs ($\text{X} = \text{V}$ or P) to CoO_x is by merely its dissolution in buffered water. It should be noted that Co_4P_2 slowly releases $\text{Co}^{2+}(\text{aq})$ upon dissolution in buffered solutions and that this process is buffer-dependent.³⁷ Early in this investigation of the CPE, the slightly soluble Cs salt of Co_4V_2 was used and despite a low solubility, growth of CoO_x from the CPE was observed upon extended BE (greater than 6 hours).

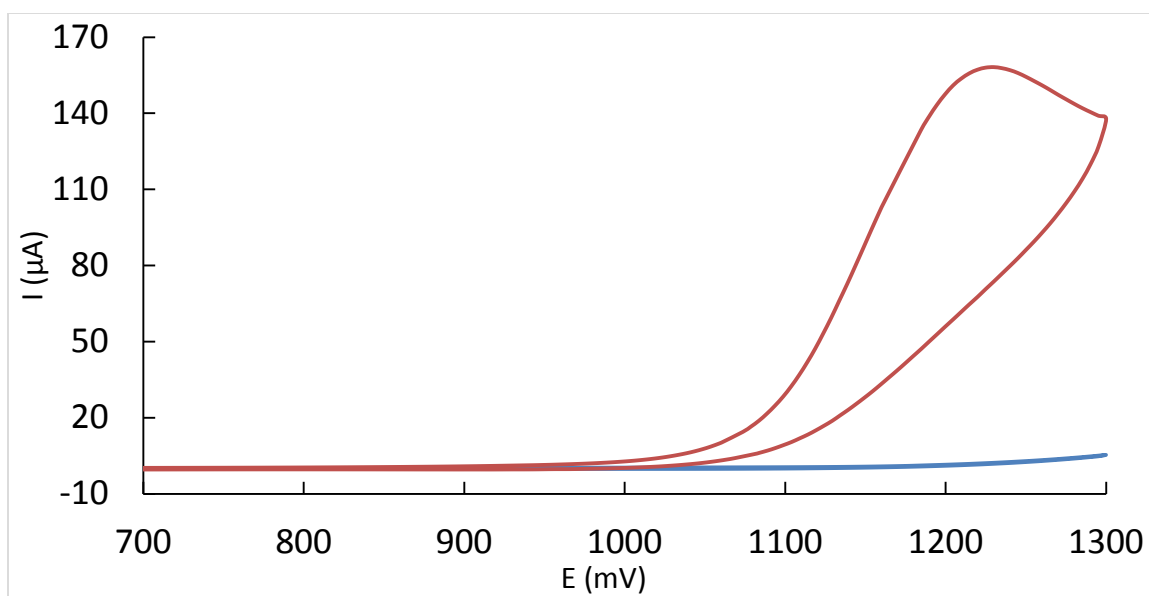


Figure 3.1. CV traces for unmodified CPE (blue) and TBA Co_4V_2 modified CPEs (red).

The CV trace of Cs Co_4V_2 (not shown) is nearly identical to that of TBA Co_4V_2 . Scan rate:

100 mV/s

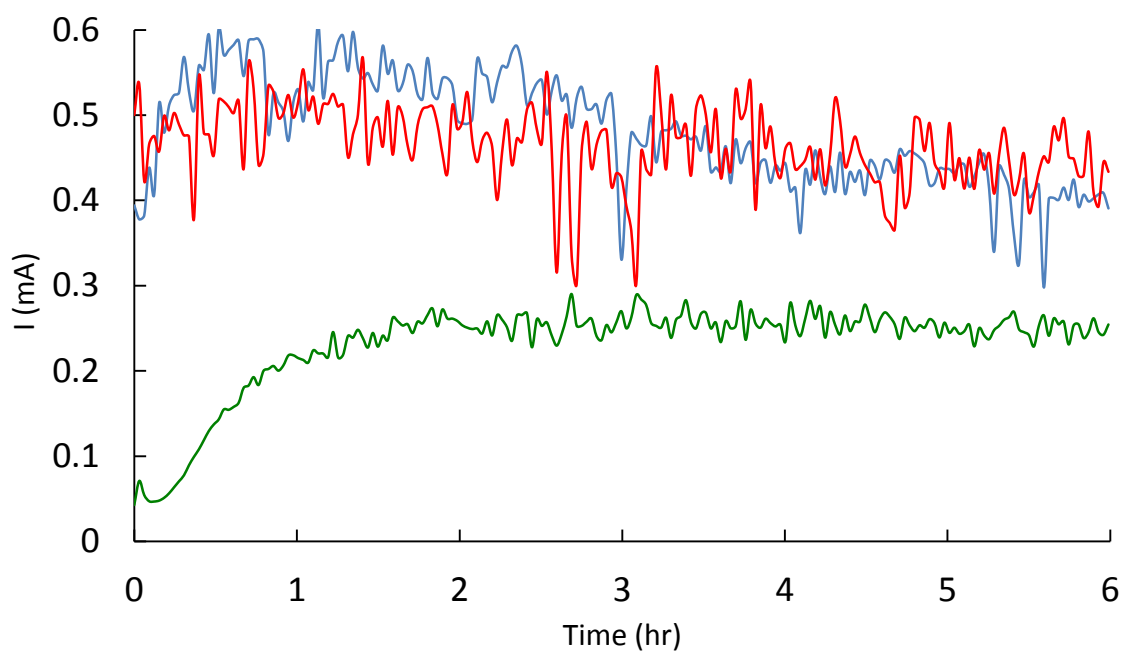


Figure 3.2. Bulk electrolyses of TBA Co_4V_2 modified CPE first run (blue), second run (red) and of an unmodified CPE (green). The large spikes in the current are due to inefficient removal of $\text{O}_{2(\text{g})}$ bubbles during the experiment.

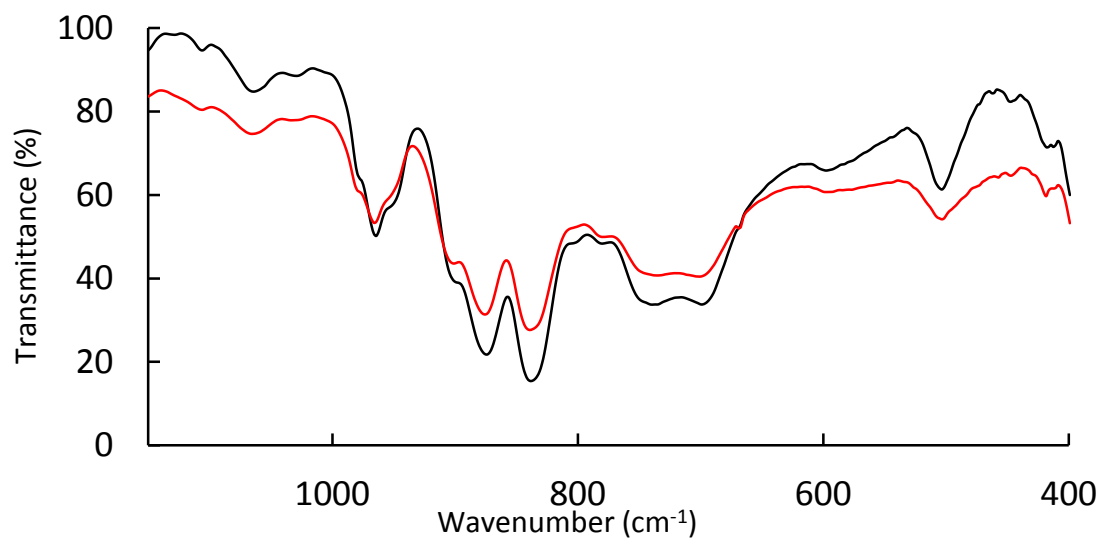


Figure 3.3. FT-IR spectra of the TBA salt of Co_4V_2 pre-BE (black) and post-BE (red), extracted from the CPE.

Another curious discovery along the way was that of the CPE electrochemically oxidizing water under the same experimental conditions employed here (Figure 3.2). Stranger still is that the Faradaic efficiency is near unity for the unmodified CPE, which begs the question, “why use a catalyst?” If the green and red traces in Figure 3.2 are compared, it becomes abundantly clear that the catalyst does increase the rate of water oxidation, thereby giving purpose to its incorporation. In direct contrast to the aforementioned report of Co_9P_5 in a CPE, no such activity was reported for the CPE alone. Another fact of interest here is that another common electrode material, glassy carbon (a different carbon allotrope), can be oxidized to carboxylate under similar conditions.⁷⁴ CPEs prepared for this study and used for water oxidation electrolysis do not appear to give the characteristic FT-IR stretches for carboxylate functional groups. Further, with a near unity Faradaic efficiency, no electrons could be spared for surface oxidation chemistry, which may be attributed to the effect that the pasting liquid, or binder, imparts on the graphite. The binder, much like the source of carbon itself, has an immense effect on the potential window of the electrode, or the voltage limits for an electrode under specified conditions.⁶⁶

In that light, some preliminary work was conducted in an attempt to hamper the CPE's ability to oxidize water under these experimental conditions. One important reason for this is that the exact sites for water oxidation at the CPE are not known, nor are of interest within the purview of the study described here. Lindquist found that ceresin, a wax derived from an odiferous paraffin, extended the potential range of CPEs.⁷⁵ Following his method⁷⁶, a batch of ceresin wax modified carbon paste was prepared and tested. A RRDE (with ring disconnected) was utilized here to compare the two CPEs, with the eventual aim to measure Faradaic efficiency, however that data will not be discussed here. In the anodic

regime, between the commercially available CPE and that of the ceresin wax modified CPE are given in Figure 3.4. A clear lower background current is observed for the ceresin wax modified CPE, which demonstrates the effect that the wax has on the electrochemical properties of the electrode. The cause of this lower background current is still not known, but could be realized through comparison of the current response to a well-known redox couple such as $[\text{Ru}(\text{NH}_3)_6]^{2+/3+}$. If the current responses were nearly identical, that would suggest that the conductivity of the paste was not affected, but rather the wax reduces the ability of graphite to oxidize water under these experimental conditions.

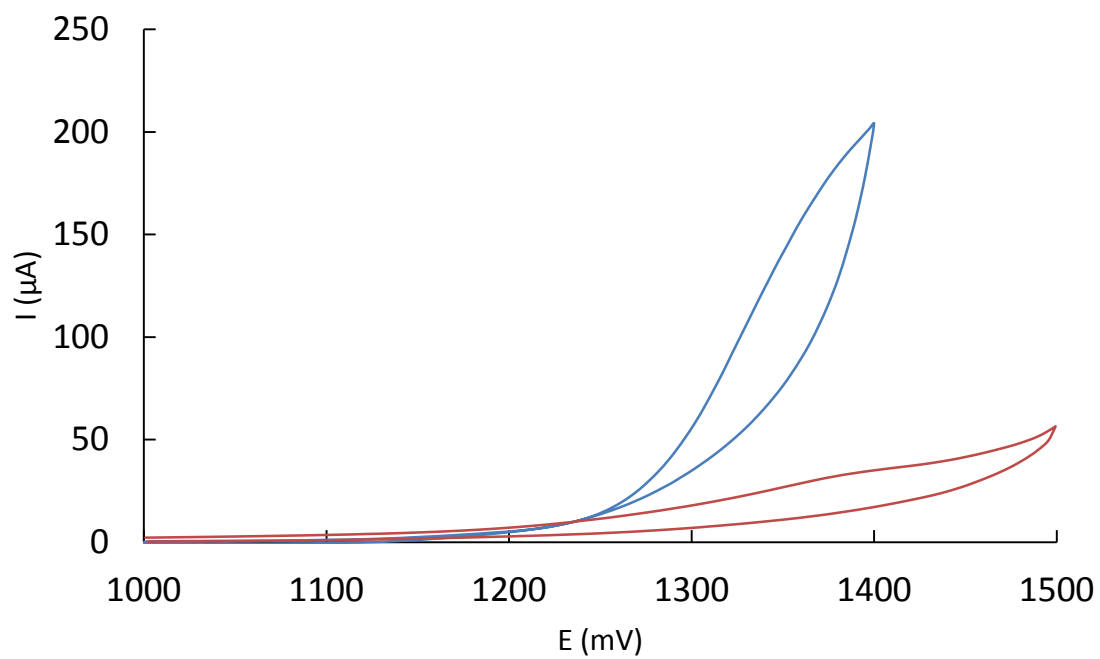


Figure 3.4. RDE CV traces of BASi CPE (blue) and ceresin wax modified CPE (red). Scan rate: 100 mV/s

Conclusions

While a Co_4V_2 modified CPE can catalyze water oxidation in an electrochemical cell, the overpotentials at which it operates are high (~ 0.75 V), which detracts from the use of these electrodes as WOC anodes in a fuel-generating cell. Since the unmodified CPE can also efficiently oxidize water under these conditions, albeit with lower activity, the nature of its activity should be investigated. However, the ultimate price for the observed activity here is through the use of high overpotentials, so a more competent catalyst that can operate at lower overpotentials (closer to the range 0.35 to 0.42 V) would vastly improve the feasibility of CPE as a WOC anode material.

References and Notes

- (1) Lewis, N. S. *MRS Bulletin* **2007**, *32*, 808.
- (2) Lewis, N. S.; Nocera, D. G. *Proc. Natl. Acad. Sci.* **2006**, *103*(43), 15729.
- (3) Blankenship, R. E.; Tiede, D. M.; Barber, J.; Brudvig, G. W.; Fleming, G.; Ghirardi, M.; Gunner, M. R.; Junge, W.; Kramer, D. M.; Melis, A.; Moore, T. A.; Moser, C. C.; Nocera, D. G.; Nozik, A. J.; Ort, D. R.; Parson, W. W.; Prince, R. C.; Sayre, R. T. *Science* **2011**, *332*, 805.
- (4) Gust, D.; Moore, T. A.; Moore, A. L. *Acc. Chem. Res.* **2009**, *42*, 1890.
- (5) Walter, M. G.; Warren, E. L.; McKone, J. R.; Boettcher, S. W.; Mi, Q.; Santori, E. A.; Lewis, N. S. *Chem. Rev.* **2010**, *110*, 6446.
- (6) Nocera, D. G. *Acc. Chem. Res.* **2012**, *45*, 767.
- (7) Huang, Z.; Xiang, C.; Lewerenz, H.-J.; Lewis, N. S. *Energy & Env. Sci.* **2014**, *2014*, 1207.
- (8) Sumliner, J. M.; Lv, H.; Fielden, J.; Geletii, Y. V.; Hill, C. L. *Eur. J. Inorg. Chem.* **2014**, *2014*, 635.
- (9) Sumliner, J. M.; Vickers, J. W.; Lv, H.; Geletii, Y. V.; Hill, C. L. In *Molecular Water Oxidation Catalysts: A Key Topic for New Sustainable Energy Conversion Schemes*; Llobet, A., Ed.; John Wiley & Sons, Ltd.: 2014 in press; Vol. First Edition, p 211.
- (10) Geletii, Y. V.; Botar, B.; Kögerler, P.; Hillesheim, D. A.; Musaev, D. G.; Hill, C. L. *Angew. Chem. Int. Ed.* **2008**, *47*, 3896.
- (11) Yin, Q.; Tan, J. M.; Besson, C.; Geletii, Y. V.; Musaev, D. G.; Kuznetsov, A. E.; Luo, Z.; Hardcastle, K. I.; Hill, C. L. *Science* **2010**, *328*, 342.
- (12) Lv, H.; Song, J.; Geletii, Y. V.; Vickers, J. W.; Sumliner, J. M.; Musaev, D. G.; Kögerler, P.; Zhuk, P. F.; Bacsa, J.; Zhu, G.; Hill, C. L. *J. Am. Chem. Soc.* **2014**, *136*, 9268.
- (13) Zhu, G.; Glass, E. N.; Zhao, C.; Lv, H.; Vickers, J. W.; Geletii, Y. V.; Musaev, D. G.; Song, J.; Hill, C. L. *Dalton Trans.* **2012**, *41*, 13043.
- (14) Lv, H.; Geletii, Y. V.; Zhao, C.; Vickers, J. W.; Zhu, G.; Luo, Z.; Song, J.; Lian, T.; Musaev, D. G.; Hill, C. L. *Chem. Soc. Rev.* **2012**, *41*, 7572.
- (15) Geletii, Y. V.; Yin, Q.; Hou, Y.; Huang, Z.; Ma, H.; Song, J.; Besson, C.; Luo, Z.; Cao, R.; O'Halloran, K. P.; Zhu, G.; Zhao, C.; Vickers, J. W.; Ding, Y.; Mohebbi, S.; Kuznetsov, A. E.; Musaev, D. G.; Lian, T.; Hill, C. L. *Isr. J. Chem.* **2011**, *51*, 238.
- (16) Pope, M. T. *Heteropoly and Isopoly Oxometalates*; Springer-Verlag: Berlin, 1983.
- (17) *Special Thematic Issue on Polyoxometalates*; Hill, C. L., Ed., 1998; Vol. 98, No. 1.
- (18) Katsoulis, D. E. *Chem. Rev.* **1998**, *98*, 359.
- (19) Sadakane, M.; Steckhan, E. *Chem. Rev.* **1998**, *98*, 219.
- (20) Pope, M. T.; Varga, G. M. *Inorg. Chem.* **1966**, *5*, 1249.

- (21) Pope, M. T.; Papaconstantinou, E. *Inorg. Chem.* **1967**, *6*, 1147.
- (22) Papaconstantinou, E.; Pope, M. T. *Inorg. Chem.* **1967**, *6*, 1152.
- (23) Varga, G. M.; Papaconstantinou, E.; Pope, M. T. *Inorg. Chem.* **1970**, *9*, 662.
- (24) Papaconstantinou, E.; Pope, M. T. *Inorg. Chem.* **1970**, *9*, 667.
- (25) Smith, D. P.; Pope, M. T. *Inorg. Chem.* **1973**, *12*, 331.
- (26) Müller, A.; Dloczik, L.; Diemann, E.; Pope, M. T. *Inorg. Chim. Acta* **1997**, *257*, 231.
- (27) Song, I. K.; Barteau, M. A. *J. Mol. Catal. A: Chem.* **2004**, *212*, 229.
- (28) Ammam, M. *J. Mater. Chem: A* **2013**, *1*, 6291.
- (29) Nadjo, L.; Keita, B. *J. Phys.* **1994**, *4*, 329.
- (30) Guo, S.-X.; Liu, Y.; Lee, C.-Y.; Bond, A. M.; Zhang, J.; Geletii, Y. V.; Hill, C. L. *Energy Environ. Sci.* **2013**, *6*, 2654.
- (31) Toma, F. M.; Sartorel, A.; Iurlo, M.; Carraro, M.; Parisse, P.; Maccato, C.; Rapino, S.; Gonzalez, B. R.; Amenitsch, H.; Ros, T. D.; Casalis, L.; Goldoni, A.; Marcaccio, M.; Scorrano, G.; Scoles, G.; Paolucci, F.; Prato, M.; Bonchio, M. *Nature Chem.* **2010**, *2*, 826.
- (32) Quintana, M.; López, A. M.; Rapino, S.; Toma, F. M.; Iurlo, M.; Carraro, M.; Sartorel, A.; Maccato, C.; Ke, X.; Bittencourt, C.; Da Ros, T.; Van Tendeloo, G.; Marcaccio, M.; Paolucci, F.; Prato, M.; Bonchio, M. *ACS Nano* **2013**, *7*, 811.
- (33) Artero, V.; Fontecave, M. *Chem. Soc. Rev.* **2012**, *42*, 2338.
- (34) Crabtree, R. H. *Chem. Rev.* **2012**, *112*, 1536.
- (35) Geletii, Y. V.; Huang, Z.; Hou, Y.; Musaev, D. G.; Lian, T.; Hill, C. L. *J. Am. Chem. Soc.* **2009**, *131*, 7522.
- (36) Stracke, J. J.; Finke, R. G. *J. Am. Chem. Soc.* **2011**, *133*, 14872.
- (37) Vickers, J. W.; Lv, H.; Sumliner, J. M.; Zhu, G.; Luo, Z.; Musaev, D. G.; Geletii, Y. V.; Hill, C. L. *J. Am. Chem. Soc.* **2013**, *135*, 14110.
- (38) Stracke, J. J.; Finke, R. G. *ACS Catal.* **2013**, *3*, 1209.
- (39) Schiwon, R.; Klingan, K.; Dau, H.; Limberg, C. *Chem. Commun.* **2014**, *50*, 100.
- (40) Ohlin, C. A.; Harley, S. J.; McAlpin, J. G.; Hocking, R. K.; Mercado, B. Q.; Johnson, R. L.; Villa, E. M.; Fidler, M. K.; Olmstead, M. M.; Spiccia, L.; Britt, R. D.; Casey, W. H. *Chem. Eur. J.* **2011**, *17*, 4408.
- (41) Lieb, D.; Zahl, A.; Wilson, E. F.; Streb, C.; Nye, L. C.; Meyer, K.; Ivanović-Burmazović, I. *Inorg. Chem.* **2011**, *50*, 9053.
- (42) Car, P.-E.; Guttentag, M.; Baldrige, K. K.; Albertoa, R.; Patzke, G. R. *Green Chem.* **2012**, *14*, 1680.
- (43) Vickers, J. W.; Sumliner, J. M.; Lv, H.; Morris, M.; Geletii, Y. V.; Hill, C. L. *Phys. Chem. Chem. Phys.* **2014**, *16*, 11942.
- (44) Lee, C.-Y.; Guo, S.-X.; Murphy, A. F.; McCormac, T.; Zhang, J.; Bond, A. M.; Zhu, G.; Hill, C. L.; Geletii, Y. V. *Inorg. Chem.* **2012**, *51*, 11521.
- (45) Goberna-Ferrón, S.; Vigara, L.; Soriano-López, J.; Galán-Mascarós, J. R. *Inorg. Chem.* **2012**, *51*, 11707.
- (46) Stracke, J. J.; Finke, R. G. *ACS Catal.* **2014**, *4*, 79.

- (47) Natali, M.; Berardi, S.; Sartorel, A.; Bonchio, M.; Campagna, S.; Scandola, F. *Chem. Commun.* **2012**, *48*, 8808.
- (48) Huang, Z.; Luo, Z.; Geletii, Y. V.; Vickers, J.; Yin, Q.; Wu, D.; Hou, Y.; Ding, Y.; Song, J.; Musaev, D. G.; Hill, C. L.; Lian, T. *J. Am. Chem. Soc.* **2011**, *133*, 2068.
- (49) Tan, M. X.; Laibinis, P. E.; Nguyen, S. T.; Kesselman, J. M.; Stanton, C. E.; Lewis, N. S. In *Prog. Inorg. Chem.*; Karlin, K. D., Ed.; John Wiley & Sons, Inc.: 1994; Vol. 41, p 21.
- (50) Cummins, D.; Boschloo, G.; Ryan, M.; Corr, D.; Rao, S. N.; Fitzmaurice, D. *J. Phys. Chem. B* **2000**, *104*, 11449.
- (51) Bird, C. L.; Kuhn, A. T. *Chem. Soc. Rev.* **1981**, *10*, 49.
- (52) Dam, H. T. v.; Ponjeé, J. J. *J. Electrochem. Soc.: Sci. Technol.* **1974**, 1555.
- (53) Kuhn, A.; Anson, F. C. *Langmuir* **1996**, *12*, 5481.
- (54) Xiang, X.; Fielden, J.; Rodríguez-Córdoba, W.; Huang, Z.; Zhang, N.; Luo, Z.; Musaev, D. G.; Lian, T.; Hill, C. L. *J. Phys. Chem. C* **2013**, *117*, 918.
- (55) Lee, M. S.; Cheon, I. C.; Kim, Y. I. *Bulletin-Korean Chemical Society* **2003**, *24*, 1155.
- (56) Bard, A. J., Faulkner, Larry R. *Electrochemical Methods: Fundamentals and Applications*; 2nd ed.; John Wiley & Sons, 2000.
- (57) Bae, E.; Choi, W.; Park, J.; Shin, H. S.; Kim, S. B.; Lee, J. S. *J. Phys. Chem. B* **2004**, *108*, 14093.
- (58) Park, H.; Bae, E.; Lee, J.-J.; Park, J.; Choi, W. *J. Phys. Chem. B* **2006**, *110*, 8740.
- (59) It is worth mentioning here the perplexing acid/base properties of this Co₄P₂, when placed in neutral or slightly basic media. Several titration experiments have been conducted to try and determine the pK_a(s) of the terminal aqua ligands on the peripheral cobalts; these data show rapid consumption of the titrant (OH⁻), followed by a slow equilibration process.
- (60) Gao, S.; Li, T.; Li, X.; Cao, R. *Mater. Lett.* **2006**, *60*, 3622.
- (61) Balula, Maria S.; Gamelas, José A.; Carapuça, Helena M.; Cavaleiro, Ana M. V.; Schlindwein, W. *Eur. J. Inorg. Chem.* **2004**, *2004*, 619.
- (62) Li, X.; She, Y.; Guo, J.; Jiang, D. *Wuli Huaxue Xuebao* **1996**, *12*, 929.
- (63) However seemingly useful P(V) might be, the viologen used here also contains it, so quantification was not performed.
- (64) Further quantification of the Faradaic efficiencies was not warranted due to the as alluded instability of this POM.
- (65) Adams, R. N. *Anal. Chem.* **1958**, *30*, 1576.
- (66) Svancara, I.; Kalcher, K.; Walcarius, A.; Vytras, K. *Electroanalysis with carbon paste electrodes*; CRC Press, 2012.
- (67) Murray, R. W. *Molecular Design of Electrode Surfaces* New York, 1992; Vol. 22.

- (68) Liu, H.; He, P.; Li, Z.; Sun, C.; Shi, L.; Liu, Y.; Zhu, G.; Li, J. *Electrochem. Commun.* **2005**, *7*, 1357.
- (69) Qu, J.; Zou, X.; Liu, B.; Dong, S. *Anal. Chim. Acta* **2007**, *599*, 51.
- (70) Soriano-López, J.; Goberna-Ferrón, S.; Vígara, L.; Carbó, J. J.; Poblet, J. M.; Galán-Mascarós, J. R. *Inorg. Chem.* **2013**, *52*, 4753.
- (71) McCrory, C. C. L.; Jung, S.; Peters, J. C.; Jaramillo, T. F. *J. Am. Chem. Soc.* **2013**, *135*, 16977.
- (72) Katsoulis, D. E.; Pope, M. T. *J. Am. Chem. Soc.* **1984**, *106*, 2737.
- (73) Hill, C. L.; Kholdeeva, O. A. In *Liquid Phase Oxidation via Heterogeneous Catalysis*; Clerici, M. G., Kholdeeva, O. A., Eds.; John Wiley & Sons, Inc.: Hoboken, New Jersey, 2013, p 263.
- (74) Kissinger, P. T.; Heineman, W. R. *Laboratory techniques in electroanalytical chemistry*; CRC press, 1996.
- (75) Lindquist, J. *Anal. Chem.* **1973**, *45*, 1006.
- (76) Atuma, S. S.; Lindquist, J. *Analyst* **1973**, *98*, 886.